The Prediction of Bubble Terminal Velocities from Wave Theory

HARVEY D. MENDELSON

Knolls Atomic Power Laboratory, Schenectady, New York

The terminal velocity of bubbles in low viscosity liquids of infinite extent is known to undergo a marked transition in behavior at an equivalent radius in the order of 0.07 cm. This transition is apparently due to a change from viscous to inviscid flow. It is also known that the inviscid flow regime can be further subdivided into surface tension- (Weber number) and buoyancy- (Froude number) dominated regimes. This behavior of rising bubbles is strikingly similar to the behavior of surface waves propagated over deep water. The analogy is found to be in quantitative agreement when the wavelength is suitably interpreted in terms of bubble dimensions. The inference of this analogy is that bubbles may be thought of as interfacial disturbances whose rate of propagation is governed by the well-known laws of wave motion.

The rise of bubbles in liquids has been extensively studied by various investigators (*1* to 5). An excellent summary of the experimental data is presented by Haberman and Morton (*1*). The data for pure water, shown in Figure 1, are typical of the rise velocity of bubbles in low viscosity liquids. The characteristic shape of this curve has generally been explained as follows:

Region 1 ($r_e < 0.035$ cm.):

In this region, the bubbles are spherical and behave as if they were solid spheres. Their terminal velocity is limited by viscous drag and they obey the Stokes law.

Region 2 (0.035 cm. $< r_e <$ 0.07 cm.):

The terminal velocity in this region is also limited by viscosity. However, due to circulation within the bubble, shear stresses at the interface are reduced and the rise velocity is greater than predicted by the Stokes law.

Region 3 (0.07 cm. $< r_e <$ 0.3 cm.):

The bubbles are no longer spherical and tend to follow a zigzag or helical path. Drag is increased by vortex formation in the wake. Peebles and Garber (*2*), using a relatively small diameter tube, found that the terminal velocity in this region could be correlated by

$$V_\infty = 1.35 \sqrt{\frac{\sigma}{r_e \rho}} \qquad (1)$$

Region 4 ($r_e > 0.3$ cm.):

Bubbles begin to assume a spherical cap shape. The analysis of Davies and Taylor (*3*) showed the terminal velocity to be

$$V_\infty = 0.67 \sqrt{g\, r_c} \qquad (2)$$

where r_c is the radius of curvature at the face of the bubble. Haberman and Morton found that, in terms of the equivalent radius, Equation (2) could be written as

$$V_\infty = 1.02 \sqrt{g\, r_e} \qquad (3)$$

Not all fluids exhibit the behavior described above. For example, the terminal velocity in highly viscous fluids may be much lower than predicted by Equations (1) and (3). However, for sufficiently large Reynolds numbers, the data approach the characteristic curve as an upper limit.

Except for the work of Davies and Taylor, little progress has been made toward a theoretical understanding of bubble motion in inviscid fluids. The major problem appears to be in describing the flow field about a bubble whose shape and trajectory are both oscillating at the same time. However, the observed analogy between waves and bubbles, described below, suggests that the fundamental mechanism involved may not be as complex as it appears at present.

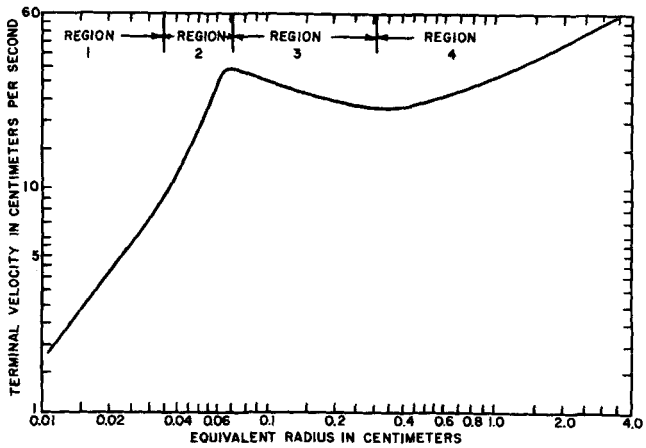

Fig. 1. Typical curve of the terminal velocity of bubbles as a function of bubble size in a low viscosity liquid.

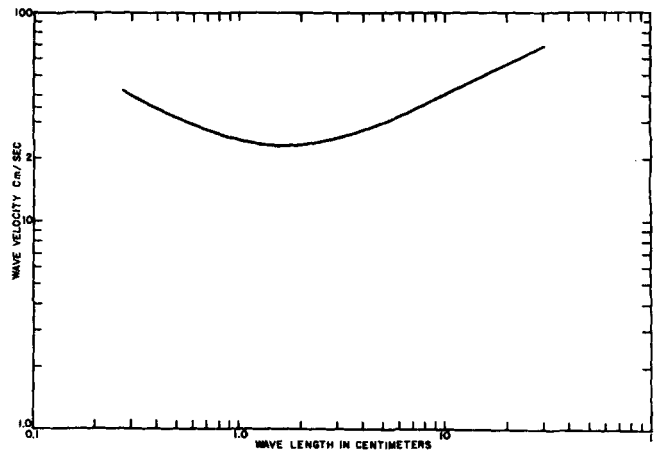

Fig. 2. Wave velocity as a function of wavelength.

THE WAVE ANALOGY

The inviscid nature of the motion of large bubbles leads to speculations that these bubbles may be thought of as merely interfacial disturbances, whose dynamic behavior should be similar to those of waves on an ideal fluid. This intuition is further supported by the similarity between the velocity of waves and the terminal velocity of large bubbles, approximately 25 cm./sec.

For waves of small wavelength compared to the depth of liquid, the wave velocity is given by reference 6.

$$c = \sqrt{\frac{2\pi\sigma}{\lambda\rho} + \frac{g\lambda}{2\pi}} \tag{4}$$

A plot of the wave velocity over water as a function of wavelength is shown in Figure 2. This curve exhibits all the characteristics of the curve for bubbles in regions 3 and 4 in that it goes through a minimum, to the left of which the motion is defined by Weber number and to the right of which the motion is defined by Froude number. The analogy becomes more obvious when the wavelength in Equation (4) is replaced by

$$\lambda = 2\pi r_e \tag{5}$$

to yield

$$V_\infty = c = \sqrt{\frac{\sigma}{r_e\rho} + g r_e} \tag{6}$$

Equation (5) (which may be thought of as defining an equivalent circumference) was obtained essentially by inspection and its only justification at present is how well Equation (6) correlates the data.

COMPARISON WITH DATA

The data presented by Haberman and Morton appear to be the most suited for testing the validity of Equation (6), since the tank used in their work was large enough to minimize wall effects. Of the thirteen fluids considered by Haberman and Morton, seven were too viscous to be applicable to the present discussion, and one contained a water solution of a surface-active agent. The data for the remaining five liquids (water, methyl alcohol, Varsol, turpentine, and a 13% solution of ethyl alcohol in water) are compared with the wave equation in Figures 3 through 7 respectively. Also shown are the data of Peebles and Garber and their correlation [Equation (1)] for region 3.

It can be seen that the wave equation adequately represents the data for region 4. This is to be expected, since

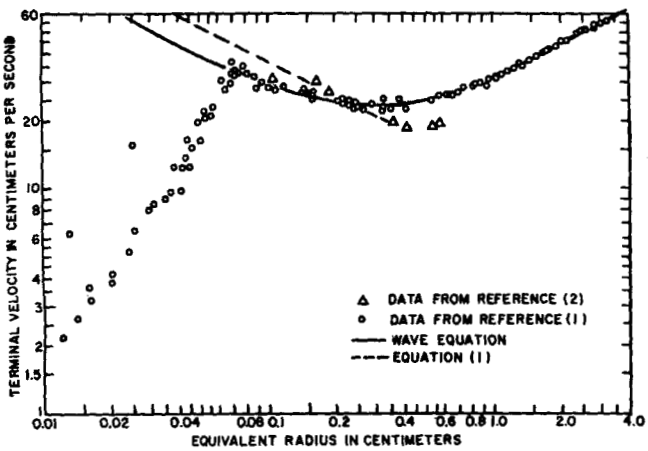

Fig. 3. Terminal velocity of air bubbles in filtered or distilled water as a function of bubble size.

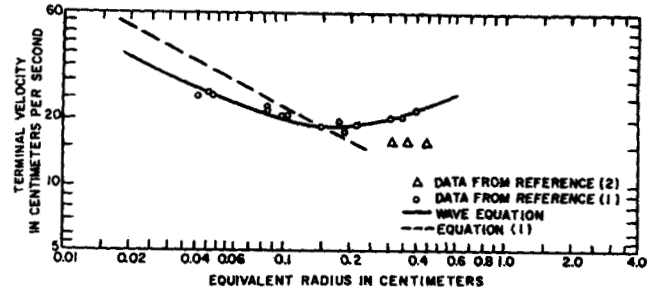

Fig. 4. Terminal velocity of air bubbles in methyl alcohol as a function of bubble size.

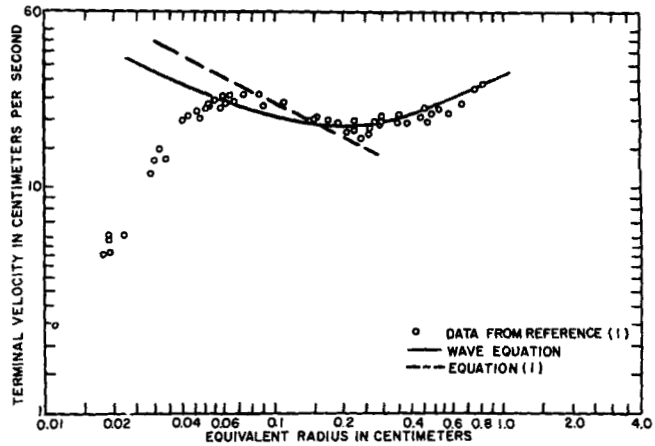

Fig. 5. Terminal velocity of air bubbles in Varsol as a function of bubble size.

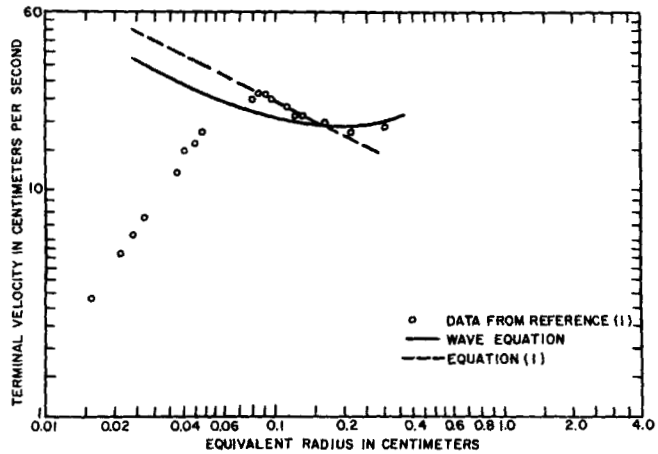

Fig. 6. Terminal velocity of air bubbles in turpentine as a function of bubble size.

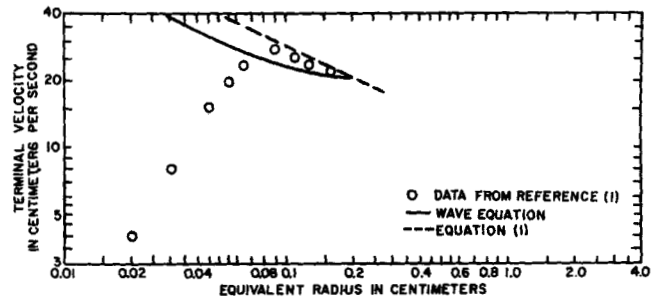

Fig. 7. Terminal velocity of air bubbles in 13% ethyl alcohol-water solution as a function of bubble size.

for large bubbles, Equation (6) reduces to Equation (2) within 2%. It may also be noted that Equation (6) is in good agreement with the data in the region of minimum rise velocity. The equation for this minimum may be obtained by setting $dc/dr_e = 0$ in Equation (6) to yield

$$V_\infty = 1.41 \sqrt[4]{\frac{\sigma g}{\rho}} \tag{7}$$

Equation (7) was obtained previously by Levich from an analysis of forces acting on a deformed bubble. Peebles and Garber recommended the equation

$$V_\infty = 1.18 \sqrt[4]{\frac{\sigma g}{\rho}}$$

to represent all of region 4. However, their data were obtained in a small diameter tube (1.03 in. I.D.) which no doubt tended to suppress the rise velocity at the minimum. They also noted the similarity of their equation to Equation (7), but their data apparently did not allow them to pursue the wave analogy further. Harmathy (5), by comparing the data for solids spheres and fluid particles, obtained the empirical correlation

$$V_\infty = 1.53 \sqrt[4]{\frac{\sigma g}{\rho}}$$

Harmathy also noted that in turbulent flow the shape of fluid particles should be a function solely of the Eötvös number and that Eötvös and Weber numbers exert an equivalent influence under these conditions. The same conclusion can be reached from the wave equation. By squaring Equation (6) and dividing by $\sigma/r_e\rho$, one obtains

$$1 + N_{E\ddot{o}} = N_{We} \tag{8}$$

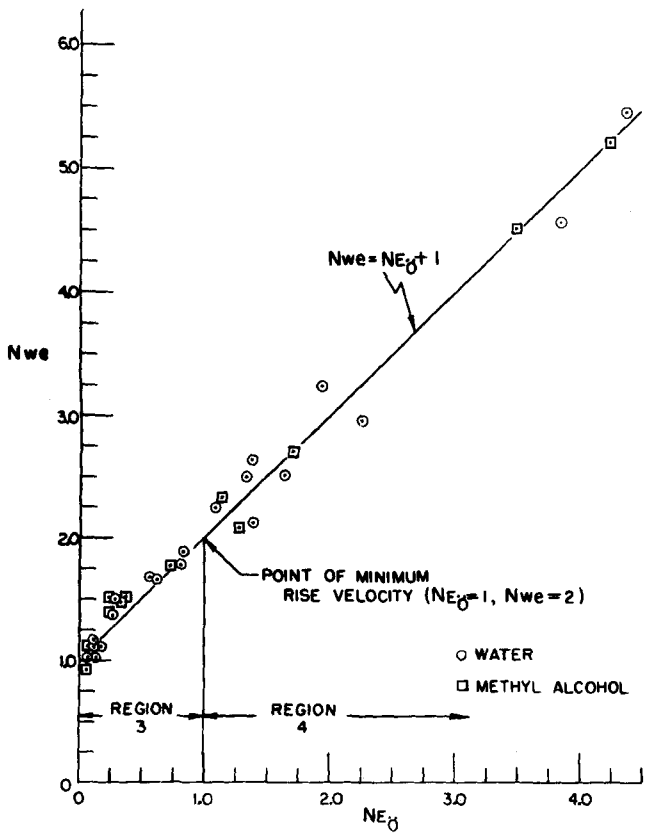

Fig. 8. Comparison of dimensionless wave equation with data of reference 1.

Thus, for large $N_{E\ddot{o}}$

$$N_{E\ddot{o}} \approx N_{We} \tag{9}$$

In region 3, the data for water and methanol tend to support Equation (6), whereas the data for the remaining liquids tend to support Equation (1). One is tempted to speculate that the difference in behavior may be due to the latter three liquids being mixtures rather than pure compounds. As such, it is conceivable that the reported surface tensions for these liquids, measured by the capillary rise method, may not be the effective surface tension at the interface of a rising bubble. Evidence to this effect is available in the literature. For example, Jontz and Myers (7) report large differences in the measured surface tension of dynamic as opposed to static interfaces. It should be noted, however, that Peebles and Garber did find Equation (1) to be applicable for many of the single-component liquids which they tested. Whether this can be attributed to a wall effect cannot be assessed without additional data. However, their data for water in region 3 are somewhat higher than those obtained by other investigators.

Equation (8), which represents a dimensionless form of the wave equation, is compared with the data for single-component liquids in Figure 8. It can be shown that the minimum terminal velocity, referred to above, occurs at $N_{E\ddot{o}} = 1$. Since the Eötvös number is the ratio of Weber number to Froude number, that is, the ratio of buoyancy to surface tension forces, the minimum velocity point occurs when these forces are equal. Thus the value $N_{E\ddot{o}} = 1$ serves to define the boundary between regions 3 and 4. These regions are indicated in the figure. Although the scatter in the data tends to be magnified by the form of the dimensionless groups, it can be seen that the wave equation represents the average of the data quite well.

CONCLUSIONS

The ability of the wave equation to predict the terminal velocity of bubbles in infinite media is significant, since it unifies the existing correlations for both the surface tension- and buoyancy-dominated regimes; furthermore, it implies that a single, and perhaps simple, mechanism determines the rise velocity of bubbles in inviscid liquids. The difficulties encountered in correlating the data for multicomponent liquids in region 3 tend to support the conclusion of other investigators that the properties at a dynamic interface may be quite different from those at a static surface.

NOTATION

c = phase velocity of surface wave, cm./sec.
g = gravitational acceleration, 981 cm./sec.^{2}
$N_{E\ddot{o}} = \frac{g\rho r_e^2}{\sigma}$, Eötvös number, dimensionless
$N_{We} = \frac{\rho r_e V_\infty^2}{\sigma}$, Weber number, dimensionless
r_c = radius of curvature of spherical cap bubble, cm.
r_e = equivalent radius of bubble, cm.
V_∞ = bubble terminal velocity, cm./sec.
λ = wavelength, cm.
ρ = density of liquid phase, g./cc.
σ = surface tension, dynes/cm.

LITERATURE CITED

1. Haberman, W. L., and R. K. Morton, *David Taylor Model Basin, NR 715-102* (Sept., 1953).

2. Peebles, F. N., and H. J. Garber, *Chem. Eng. Progr.*, **49**, 2 (Feb., 1953).
3. Davies, R. M., and G. Taylor, *Proc. Royal Soc. (London)*, **200A**, 375-390 (1950).
4. Levich, V. G., "Physicochemical Hydrodynamics," Prentice-Hall, Englewood Cliffs, N. J. (1962).
5. Harmathy, T. Z., *A.I.Ch.E. J.*, **6**, No. 2, 281 (1960).
6. Lamb, H., "Hydrodynamics," 6 ed., Dover, New York (1932).
7. Jontz, P. D., and J. E. Myers, *A.I.Ch.E. J.*, **6**, No. 34 (1960).

Manuscript received August 18, 1966; revision received November 29, 1966; paper accepted December 1, 1966.

Flow of Viscoelastic Fluids Past a Flat Plate

R. A. HERMES and A. G. FREDRICKSON

University of Minnesota, Minneapolis, Minnesota

The flow of viscoelastic fluids past a flat plate has been investigated. Experimental studies were performed with aqueous solutions of sodium carboxymethylcellulose used as viscoelastic fluids and corn syrup as a viscous Newtonian fluid. It was observed that the flow patterns of elastic and inelastic fluids are markedly different. Tracer particles placed in the approaching viscoelastic fluids to follow their motion were seen to first decelerate and then to accelerate until a nearly constant velocity was reached. On the other hand tracer particles in the Newtonian fluid were observed merely to decelerate smoothly to the constant velocity.

The drag force measured for the viscoelastic fluids was found to be roughly twice that predicted by inelastic models of fluid behavior. Predicted and measured values of the drag force for the Newtonian fluid agreed well.

A discussion of mathematical solutions to the problem of flow of viscoelastic fluids past a flat plate is given. Solutions are obtained for a prototype of flow past a flat plate, the suddenly accelerated flat plate (Stokes' problem) with linear viscoelastic models used. The results from Stokes' problem qualitatively explain the anomalous kinematical behavior and the large drag force.

Many important commercial processes involve the flow of viscoelastic fluids in complex geometries. Although very general constitutive equations have been provided for these fluids (*6, 7, 10*), few engineering problems using them have been solved. The problem considered in this paper is flow of viscoelastic fluids past a flat plate, a prototype of many flow situations encountered in industry. Studies of complex flow situations are important from a fundamental viewpoint also. For viscometric flows the general theory of Coleman and Noll (*6*) can be shown to reduce to the determination of three material functions: a viscosity function and two normal stress differences (*7*). The simple degeneracy of these flows comes about because the kinematical history of a material particle is the same for all past times within its memory. Methods are described in the literature for the measurement of all three of these material functions (*9, 12, 17, 21*). The next step in elucidating the nature of viscoelastic fluids seems to be the study of complex flows where at least some of the degeneracy of laminar shear flows is removed.

Recent results on steady complex flows of non-Newtonian fluids that display viscoelastic properties show conflicting results. In some situations it has been found that solutions of the equations of motion using inelastic, non-Newtonian models are sufficient to describe macroscopic variables of primary engineering interest. For example, Sutterby (*29*) found that laminar converging flow in a conical section could be described by a non-Newtonian, inelastic model he proposed. Likewise Sadowski (*23*) has shown that his data on flow in a packed bed could be described by using the Ellis model. On the other hand, Walters and Savins (*26*) have shown that the flow patterns around a rotating sphere are qualitatively different for a viscoelastic fluid than for an inelastic fluid. Sakiadis (*24, 25*) has done experimental studies on entrance effects into a capillary and found larger pressure losses and a longer entrance length than predicted by inelastic theory. Many other examples could be cited, of course. However, no definite method of predicting the importance of elastic effects a priori has been given. However, one can probably say that the longest relaxation time of the fluid must be of the same order or greater than some characteristic time of the system, if elastic effects are to be of importance. More experimental and theoretical work is needed to establish the conditions under which viscoelastic effects are important.

Recently, attention has been turned to flow past submerged objects (*19, 31*). These flows are important from a fundamental standpoint because they are unsteady in the Lagrangian sense. That is, the kinematic state viewed by a material particle changes as it traverses the object. It is in these flows in which the kinematic history of a material particle changes with time that elastic effects are usually manifested.

THEORY

The problem of flow of purely viscous fluids past a flat plate (boundary-layer flow) has been studied in detail. For Newtonian fluids many solutions, both exact and approximate, are available (*27*). Acrivos et al. (*1, 2*) and Schowalter (*28*) have analyzed this problem for fluids which obey the power law model

R. A. Hermes is with Mobil Oil Corporation, Dallas, Texas.